Proceedings of Meetings on Acoustics

Volume 11, 2010 http://acousticalsociety.org/

160th Meeting
Acoustical Society of America
Cancun, Mexico
15 - 19 November 2010
Session 1pNS: Noise

1pNS5. On near-field acoustical inverse measurements of partially coherent sources

Alan T. Wall*, Kent L. Gee, Tracianne B. Neilsen and Michael M. James

***Corresponding author's address: Department of Physics and Astronomy, Brigham Young University, N283 ESC, Provo, Utah 84663, alantwall@gmail.com**

The sources of jet noise have been investigated through the use of near-field array measurements. An understanding of spatial coherence properties in the jet near field leads to insight about source composition. A metric called coherence length is a useful tool for summarizing near-field coherence information. Near-field coherence lengths are presented in this work for a full-scale jet, which show that jet noise is composed of two distinct components: (1) highly spatially coherent, low-frequency, large-scale turbulent structures and (2) high-frequency fine-scale turbulence with very low spatial coherence. The spatial extent and coherence of jet noise sources support the use of near-field acoustical holography as a viable jet-noise-source imaging technique.

Published by the Acoustical Society of America through the American Institute of Physics

 [DOI: 10.1121/1.4726051]
Received 20 Feb 2012; published 21 May 2012

I. INTRODUCTION[a]

Near-field coherence measurements can lead to a greater understanding of a source when its properties are unknown, such as in aeroacoustic noise. Accurate characterization of noise sources within a jet provides insight into physical noise generation mechanisms in the turbulent flow field. This characterization can help lead to reduction of the noise that causes significant hearing loss in military personnel and is a disturbance to communities. Although the results presented here are nearly identical to those presented at the 160th Meeting of the Acoustical Society of America in a talk entitled "Considerations for near-field acoustical inverse measurements on partially correlated sources," there is a slight shift in focus from the presented talk to this paper. This change in focus is reflected in the two respective abstracts.

Jet noise is predominantly represented with two distinct source types: fine-scale turbulence structures and large-scale turbulence structures.[1-3] The fine-scale turbulence tends to be made of many independent structures that radiate sound omnidirectionally. However, there is significant spatial coherence along the jet axis due to the physical extent of the large-scale structures, particularly at low frequencies.[4] This leads to highly coherent, directional noise radiation.

The large spatial extent of these sources has important implications for the type of acoustic measurement performed. Acoustical inverse methods, such beamforming[5,6] and other far-field methods,[1,7,8] have often been employed to measure source strengths, size, and distribution within the turbulent flow. However, these methods have been shown to perform poorly for spatially noncompact, correlated sources.[9,10] Therefore, near-field acoustical holography (NAH) is being explored as an alternative jet noise visualization technique.[11-14]

The purpose of this paper is to address the utility of measuring coherence length—a metric that summarizes spatial coherence information—in the geometric near field of jet noise sources. Coherence lengths measured in the near field of the jet plume from an F-22A Raptor are presented here. They are compared to the coherence lengths of a numerical line array of uncorrelated simple sources. These data reveal important source coherence properties. Additionally, they demonstrate the utility of NAH measurements on jet noise sources.

II. THEORY

A useful metric for examining near-field coherence is the coherence length, here defined as the distance (parallel to the extent of a long source) over which the coherence function, γ^2,[15] drops from unity to a value of 0.5.[16,17] To determine the coherence length, L_C, the coherence between a single reference transducer and all other transducers in a linear array are calculated. The physical distance between the reference transducer and the transducer (in the upstream direction of propagation) at which coherence falls below 0.5 is L_C, and this value is assigned to the physical location of the reference transducer.

For example, if the coherence function across an array varies like a Rayleigh curve, as shown in Figure 1, then L_C is given by the distance indicated, which is about 2 m. As is often the case, a coherence length can be calculated in the two opposite directions. When this occurs, the value measured in one direction or the other, or an average of these two values can be used to

[a] SBIR DATA RIGHTS. Distribution A – Approved for Public Release; Distribution is Unlimited 88ABW-2012-2280. (See Acknowledgments for full statement.)

determine the coherence length.[18] Here, in this work, L_C is defined in the direction of decreasing x.

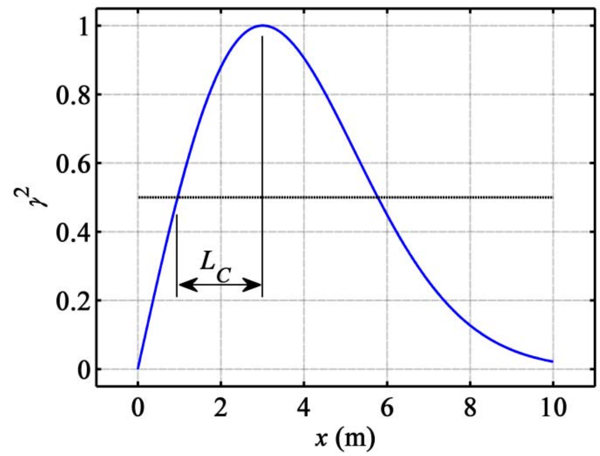

Figure 1 An example coherence length measurement, L_C, for an arbitrary spatial coherence measurement referenced to a signal at $x = 3$ m.

III. EXPERIMENT

A brief summary of the measurement—focusing on the ground-based microphone array—is given here. A more complete description of the holographic measurement is provided in References 19 and 20. In July 2009, near-field measurements of the jet on a Lockheed Martin/Boeing F-22 Raptor were taken at Holloman Air Force Base in New Mexico. Fifty microphones (shown in Figure 2) were placed on the ground with 0.61 m (2 ft.) spacing, spanning more than 30 m and running parallel to the jet flow at a perpendicular distance of 11.7 m from the jet centerline. A top-view schematic of the location of the microphone array relative to the aircraft and jet is shown in Figure 3. Complex sound pressures were measured over a broad range of frequencies, and from these L_C values were calculated at all measurement locations along the array.

Figure 2 Close-up of several ground-based microphones placed at a perpendicular distance of 11.7 m from the centerline of the jet on an F-22 Raptor. The array spanned more than 30 m.

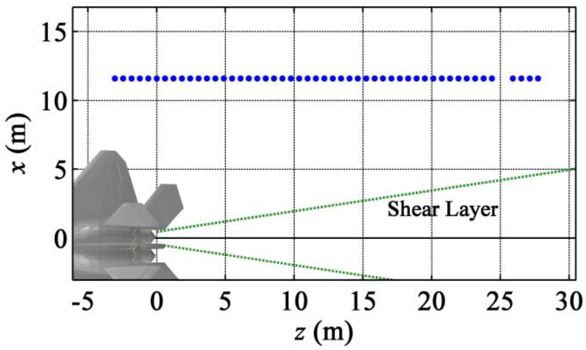

Figure 3 Top view schematic of the microphone array location relative to the jet. Microphone locations are marked by blue dots. The array is located 11.7 m from the jet centerline.

A second experiment was performed on an extended numerical source. This source was not designed to model actual jet noise, but rather to draw a comparison between near-field coherence properties of the jet and an uncorrelated source array. The source was comprised of a line array of 151 uncorrelated monopoles at a height of $y = 1.9$ m, spaced 0.1 m apart (closely spaced relative to wavelengths of interest) and extending from 0 to 15 m in the positive z direction. This corresponds to the location of the jet centerline on the F-22 Raptor, as shown in Figure 4. The measured sound pressures were simulated in the same relative locations as the ground-based microphone array using propagation via the free-space Green's function. Similar to the physical experiment, L_C values were calculated at all measurement locations along the simulated array.

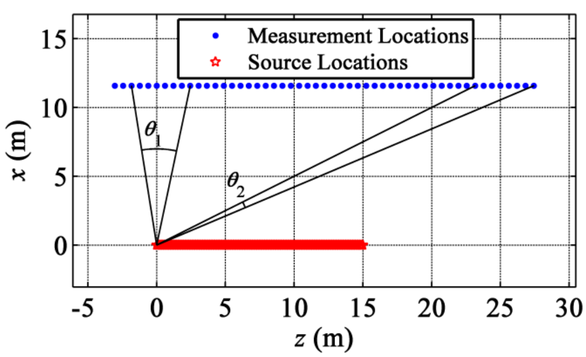

Figure 4 Top view schematic of the measurement array location relative to the uncorrelated line array of 151 monopoles. Measurement locations are marked by blue dots. The array is located 11.7 m from the source array.

IV. RESULTS

Coherence function values, γ^2, were calculated across the measurement array referenced to the signal measured by a single transducer on the array at $z = 14.6$ m. The aircraft was operating at military engine conditions. The values calculated for γ^2 at 120 Hz are shown in Figure 5. These data represent well the trends seen in all near-field γ^2 measurements of the jet: coherence decays away from the reference location and the curve is typically asymmetric. The resulting coherence length of $L_C = 5.7$ m, assigned to this frequency and location, is also illustrated.

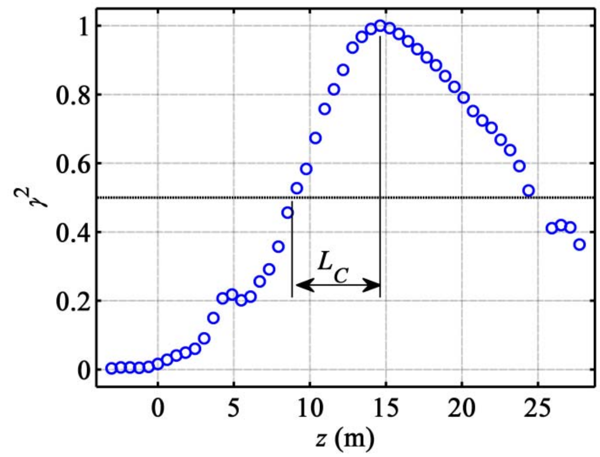

Figure 5 Coherence values at 120 Hz calculated between the signal measured at z = 14.6 m and all measurements along the microphone array with the aircraft operating at military engine conditions. The physical distance representing the coherence length of 5.7 m, assigned to the transducer at z = 14.6 m, is marked.

The sound pressure levels (SPLs) over a broad range of narrowband frequencies, measured along the microphone array, are shown in Figure 6a. The respective L_C values are plotted in Figure 6b. Note that the L_C values tend to increase both with decreasing frequency and greater distance downstream (larger z). Coherence lengths are very large—greater than 10 m—beyond $z = 20$ m and below about 130 Hz. The regions of largest L_C values in Figure 6b tend to correspond to the regions of highest SPL in Figure 6a.

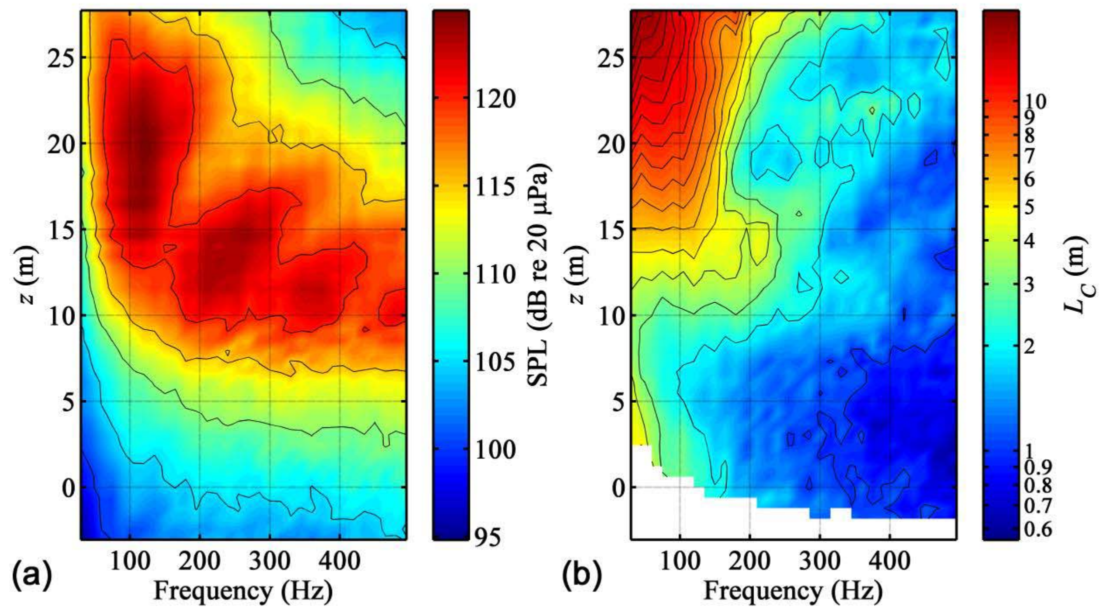

Figure 6 (a) SPLs measured by the ground-based microphone array running parallel to and 11.7 m from the centerline of the jet on the F-22 Raptor, operating at military engine conditions. (b) Calculated coherence lengths along the microphone array.

Long, coherent sources lead to large coherence length measurements in the geometric near field. The high spatial extent of the large-scale turbulence structures predicted in the two-source model[4] is therefore reflected in the regions of large L_C at low frequencies, shown in Figure 6b. This suggests that the lowest frequency sources, likely generated by the large-scale turbulence structures, exhibit the highest spatial coherence.

While the general trend is that L_C increases gradually with distance downstream, there is an uncharacteristically sharp rise in L_C near $z = 15$ m for all frequencies below 200 Hz in Figure 6b. There are also high levels measured below 200 Hz and past $z = 15$ m, displayed in Figure 6a. This is probably because the large-scale structures tend to radiate in a preferred downstream direction that is fairly constant over this frequency range.[21]

It is instructive to consider the two limits of spatial source coherence, and their effect on the radiated sound field. First, a perfectly coherent source produces a perfectly coherent field, resulting in an infinite coherence length at all locations. The numerical experiment on an array of completely independent sources provides an example of the opposite limiting case. Again, SPLs are shown over a broad range of frequencies along the array (see Figure 7a), and the respective L_C values are plotted in Figure 7b. Between these two extremes lies the case of a partially correlated source.

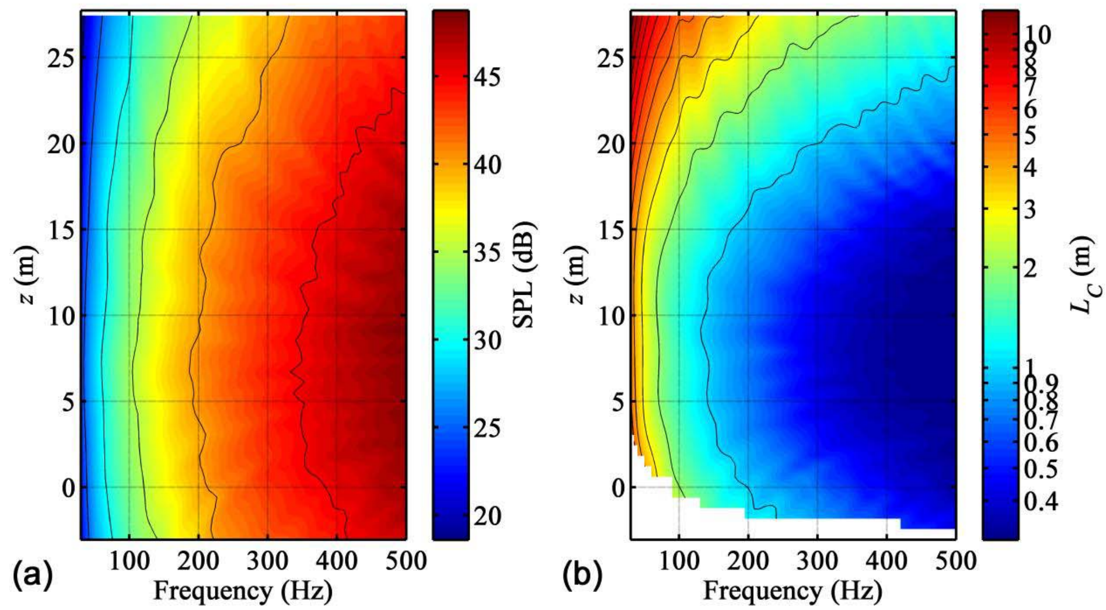

Figure 7 (a) SPLs measured by the simulated microphone array running parallel to and 11.7 m from the numerical source array. (b) Calculated coherence lengths along the simulated measurement array.

As with the jet data, L_C for the numerical source, shown in Figure 7b, tends to increase as frequency decreases and with increasing distance "downstream." Since the overall trends in L_C values for the uncorrelated numerical case match those of the jet data, the majority of the radiated jet-noise field above about 200 Hz and upstream of $z = 15$ m is probably generated by sources of low spatial coherence, i.e. fine-scale turbulence.

An important difference in the numerical experiment is that there is no abrupt onset of high L_C values at $z = 15$ m. Trends over all frequencies and locations vary smoothly. Since the numerical source is spatially incoherent, this further supports the idea that the low-frequency, downstream region of the jet with anomalously high L_C values is dominated by radiation from a spatially coherent source.

Note that regions of small L_C values in Figure 7b tend to correspond to the regions of maximum SPL in Figure 7a. This is the opposite of the trend seen in highly coherent portions of the jet noise data shown in Figure 6. The sources are independent, so they exhibit no radiation directionality. Therefore, for all frequencies, the maximum SPL and shortest L_C occur at $z = 7.5$ m, which location corresponds to the center of the source array. All levels and coherence lengths at other locations are symmetric about this central distance.

An important factor influencing the values of L_C is the fact that microphones near the end of the array are receiving the signal "end on" from a long, narrow source region. In other words, the arriving signal approaches a grazing incidence along the array far downstream. Figure 4 illustrates this concept. Here, two sets of eight microphones are selected from the simulated measurement array: one set near the first source and another far downstream. The angle θ_2 "covered" by the latter set is significantly smaller than the angle θ_1 covered by the former. The result is that L_C values increase with distance from the source region as a result of simple geometry, independent of source coherence.

The effects of measurement geometry—isolated from the effects of source coherence—are further demonstrated by the numerical experiment. Recall that the source is composed of a series of uncorrelated monopoles. Therefore, the increase of L_C with distance downstream in Figure 7b is a result of geometry. It is important to realize that measurement geometry effects must be carefully considered when using near-field coherence lengths to make inferences about source coherence properties. This does not rule out using L_C as an indicator of source coherence. On the contrary, the large yet finite coherence lengths below 200 Hz and past $z = 15$ m in Figure 6b point directly to a partially coherent source.

V. IMPLICATIONS FOR NAH

Sound pressure measurements made in the acoustic far-field (much farther from the source than a wavelength) cannot resolve individual sources spaced closer together than one half of a wavelength. Fuchs[9] shows that applying far-field measurement techniques to sources with large spatial coherence can lead to misleading source distributions and poor estimates of localized sound power. Venkatesh[10] explains that phased-array techniques like beamforming, which work well in locating a set of multiple, isolated point sources, can perform poorly when reconstructing extended noise sources. Therefore, the effectiveness of the popular beamforming and other far-field techniques for jet-noise studies is questionable.

Because NAH requires no restrictions on source composition, it can be implemented effectively for sources composed of distinct or extended, coherent or incoherent subsources. Much of jet noise is generated by extended, partially coherent sources. This potentially makes NAH a promising alternative to other acoustical inverse methods for jet-noise characterization.

VII. CONCLUSIONS

Coherence length values have been reported for a full-scale jet, installed on a military aircraft. The changes in L_C as a function of frequency and distance downstream support the two-source representation of jet noise. Values of L_C are very long at low frequencies in the downstream region, but remain relatively short for high frequencies and farther upstream. These provide evidence of the large-scale and fine-scale components of jet noise, respectively. The analyses presented demonstrate the utility of the coherence length L_C, as it is defined here, in summarizing near-field spatial coherence and making inferences about spatial source coherence. However, it is important to consider the effects of measurement array location when making such inferences. The spatial extent and high coherence of jet noise sources also point toward near-field acoustical holography as a preferred jet-noise measurement technique.

ACKNOWLEDGMENTS

This research was supported in part by the appointment of Alan Wall to the Student Research Participation Program at U.S. Air Force Research Laboratory, Human Effectiveness Directorate, Warfighter Interface Division, Battlespace Acoustics administered by the Oak Ridge Institute for Science and Education through an interagency agreement between the U.S. Department of Energy and USAFRL.

SBIR DATA RIGHTS - (DFARS 252.227-7018 (JUNE 1995)); Contract Number: FA8650-08-C-6843; Contractor Name & Address: Blue Ridge Research and

[1] J. Laufer, R. Schlinker and R. E. Kaplan, "Experiments on supersonic jet noise," AIAA J. **14**, 489-497 (1976).
[2] C. K. W. Tam, "Jet noise: Since 1952," Theoretical and Computational Fluid Dynamics **10**, 393-405 (1998).
[3] K. Viswanathan, "Mechanisms of jet noise generation: Classical theories and recent developments," International Journal of Aeroacoustics **8**, 355-408 (2009).
[4] C. K. W. Tam, K. Viswanathan, K. K. Ahuja and J. Panda, "The sources of jet noise: Experimental evidence," J. Fluid Mech. **615**, 253-292 (2008).
[5] B. D. Van Veen and K. M. Buckley, "Beamforming: A versatile approach to spatial filtering," IEEE ASSP Magazine, 4-24 (1988).
[6] R. H. Schlinker, S. A. Liljenberg, D. R. Polak, K. A. Post, C. T. Chipman and A. M. Stern, "Supersonic jet noise source characteristics & propagation: Engine and model scale," AIAA Paper 2007-3623, May 21-23, 2007.
[7] J. Billingsley and R. Kinns, "The acoustic telescope," J. Sound Vib. **48**, 485-510 (1976).
[8] M. J. Fisher, M. Harper-Bourne and S. A. L. Glegg, "Jet engine noise source location: The polar correlation technique," J. Sound Vib. **51**, 23-54 (1977).
[9] H. V. Fuchs, "On the application of acoustic 'mirror', 'telescope', and 'polar correlation' techniques to jet noise source location," J. Sound Vib. **58**, 117-126 (1978).
[10] S. R. Venkatesh, D. R. Polak and S. Narayanan, "Beamforming algorithm for distributed noise source localization and its application to jet noise," AIAA J. **41**, 1238-1246 (2003).
[11] M. Lee and J. S. Bolton, "Source characterization of a subsonic jet by using near-field acoustical holography," J. Acoust. Soc. Am. **121**, 967-977 (2007).
[12] A. T. Wall, K. L. Gee, M. D. Gardner, T. B. Neilsen and M. M. James, "Near-field acoustical holography applied to high-performance jet aircraft noise," Proc. Mtgs. Acoust. **9**, 040009 (2011).
[13] P. N. Shah, H. Vold and M. Yang, "Reconstruction of far-field noise using multireference acosutical holography measurements of high-speed jets," AIAA Paper 2011-2772, June 5-8, 2011.
[14] H. Vold, P. N. Shah, J. Davis, P. G. Bremner, D. McLaughlin, P. Morris, J. Veltin and R. McKinley, "High-resolution continuous scan acoustical holography applied to high-speed jet noise," AIAA Paper 2010-3754, June 7-9, 2010.
[15] J. S. Bendat and A. G. Piersol, *Random data: Analysis and measurement procedures*, Fourth ed. (John Wiley & Sons, Inc., Hoboken, New Jersey, 2010).
[16] M. Gardner, *Scan-based near-field acoustical holography on partially correlated sources* (M.S. Thesis, Brigham Young Univ., Provo, UT, 2009).
[17] J. M. Collis, T. F. Duda, J. F. Lynch and H. A. DeFerrari, "Observed limiting cases of horizontal field coherence and array performance in a time-varying internal wavefield," J. Acoust. Soc. Am. **124**, EL97-EL103 (2008).
[18] In a previous conference proceedings (see Reference 12) the average value was used.

[19] M. M. James and K. L. Gee, "Aircraft jet plume source noise mesurement system," Sound Vib. **44**, 14-17 (2010).
[20] A. T. Wall, K. L. Gee, M. M. James, K. A. Bradley, S. A. McInerny and T. B. Neilsen, "Near-field noise measurements of a high-performance military jet aircraft," Noise Control Eng. J., (submitted 2012).
[21] C. K. W. Tam, "Mach wave radiation from high-speed jets," AIAA J. **47**, 2440-2448 (2009).
[22] E. G. Williams, *Fourier acoustics: Sound radiation and nearfield acoustical holography* (Academic Press, San Diego, 1999).